Journal of Inorganic and General Chemistry
ZAAC
Zeitschrift für anorganische und allgemeine Chemie
DOI: 10.1002/zaac.201900310
ARTICLE

Iron(II) Complexes of Chiral Tridentate Nitrogen Donors and their Application in Catalytic Hydrosilylation Reactions

Cedric Groß,[a] Andreas Omlor,[b] Tobias Grimm,[a] Benjamin Oelkers,[a] Yu Sun,[a] Volker Schünemann,[b] and Werner R. Thiel*[a]

Dedicated to Prof. Dr. Manfred Scheer on the Occasion of his 65th Birthday

Abstract. Enantiomerically pure, C_2-symmetric 2,6-bis(pyrazol-3-yl) pyridine ligands were obtained by treatment of diethyl-2,6-pyridinedicarbonate with (1*R*,4*R*)-(+)-camphor in the presence of NaH followed by ring closure with hydrazine. After twofold N-alkylation at the pyrazole rings, the addition of iron(II) chloride led to the according pentacoordinate dichloridoiron(II) complexes. All intermediates of the ligand synthesis, the ligands bearing NCH_3 and $NCH_2C_6H_5$ groups and the derived iron(II) complexes were structurally characterized by means of X-ray structure analysis. In-situ reaction with iron(II) carboxylates resulted in the formation of iron(II) carboxylate complexes, which turned out to be highly active in the hydrosilylation of acetophenone. However, even at room temperature, the enantiomeric excess of the product 1-phenylethanol is poor. ^{57}Fe Mössbauer spectroscopy gave an insight into the species formed during catalysis.

Introduction

One of the twelve principles of "Green Chemistry" is to perform reactions under catalytic conditions which saves energy and leads to smaller amounts of undesirable side products.[1] However, most applications of transition metals as catalysts were reported in the past used expensive and often toxic noble metals.[2] During the last decade, more and more of the earth abundant 1st row transition metals such as copper, nickel, cobalt or iron, which have been well-known for long as reaction centers in the catalytically active sites of metallo enzymes, were investigated for their performance in classical catalytic transformations.[3] Especially inexpensive and largely biocompatible iron complexes have turned out to be able to offer a wide range of possible applications in catalysis[4] in addition to the often interesting electrochemical and photo-physical features of such compounds.[5] As its heavier homologue ruthenium, iron is able to catalyze hydrogenation and transfer hydrogenation reactions. *Morris* et al. could show that tetradentate *P,N,N,P* donors are ideal ligands to stabilize the iron sites for these transformations.[6] Another important class of iron catalysts based on bulky 2,6-diiminopyridines was independently from each other published some years earlier by Gibson and Brookhart for ethylene polymerization.[7] A particularly promising field for iron catalysis is catalytic hydrosilylation with either chiral[8] or achiral[9] iron(II) complexes.

Compared to ruthenium(II) compounds, typical iron(II) complexes are kinetically less stable. Therefore multidentate ligands such as the above-mentioned *P,N,N,P* systems or terpyridine ligands[10] are requested to guarantee a minimum of structural stability. However, it is difficult to achieve a broad variety of structurally closely related donors from tridentate *N,N,N* ligands like terpyridines since pyridines are deactivated aromatic systems and thus not prone for example to electrophilic substitution. Nevertheless, the systematic variation of the electronic and steric impact of a ligand structure provides an elegant way to elucidate structure/activity relationships in catalysis and in consequence to optimize a catalyst. We therefore looked for an alternative for the terpyridine structure and found 2,6-bis(pyrazol-3-yl)pyridines to be a perfect motif for applications and mechanistic investigations in catalytic reactions.[11] Chemical functionalization of 2,6-bis(pyrazol-3-yl) pyridines can readily be achieved by a number of established synthesis protocols.[12] The pyrazole rings are formed by a condensation reaction between hydrazine and functionalized 1,3-diketones. Pyrazoles are activated aromatic systems which can further be functionalized by electrophilic aromatic substitution reactions.

1,3-Diketones are accessible e.g. by condensation reactions starting from an ester and a ketone or an aldehyde. It therefore is possible to get access to chiral 2,6-bis(pyrazol-3-yl)pyridine derivatives by either taking an ester of a chiral carboxylic acid or a chiral ketone/aldehyde. Since we frequently started from pyridine-2,6-dicarboxylic acid to build up the 2,6-bis(pyrazol-3-yl)pyridines in the past, we decided to introduce a chiral

* Prof. Dr. W. R. Thiel
E-Mail: thiel@chemie.uni-kl.de
[a] Fachbereich Chemie
Technische Universität Kaiserslautern
Erwin-Schrödinger-Straße 54
67663 Kaiserslautern, Germany
[b] Fachbereich Physik
Technische Universität Kaiserslautern
Erwin-Schrödinger-Straße 56
67663 Kaiserslautern, Germany
Supporting information for this article is available on the WWW under **http://dx.doi.org/10.1002/zaac.201900310** or from the author.

ketone to get access to enantiomerically pure tridentate *N*,*N*,*N* donors. Such ligands may find application in asymmetric hydrosilylation,[13] alkene epoxidation and aziridination reactions.[14] In order to increase the stereoselectivity of a catalytic reaction it is advantageous to reduce the number of possible ligand conformations and of catalyst-substrate interactions by creating C_2-symmetric catalysts.[15] Based on this, *Steel* et al. developed chiral heterocyclic ligands derived from camphor, among them C_2-symmetric 2,6-bis(pyrazol-1-yl)pyridines wherein the pyrazole rings were directly bound to the pyridine ring by one of their nitrogen atoms.[16] However, to the best of our knowledge, C_2-symmetric 2,6-bis(pyrazol-3-yl)pyridines, wherein the pyrazoles are connected to the pyridine ring by C–C bonds are yet unknown. These ligands provide another position for functionalization: the pyrazole NH moiety can e.g. be used to introduce long alkyl chains to simply increase the catalysts' solubility in non-polar solvents[17] or to introduce side chains that allow immobilizing the catalyst covalently onto an oxidic surface of a support material.[18]

Hydrosilylation is the addition of a silylhydride to an unsaturated system. In case of carbonyl compounds silylethers are obtained as the products, which are rather reactive and can be easily converted to alcohols under basic conditions.[19] In the last decades different homogeneous catalysts often containing transition metal sites were found to catalyze hydrosilylation reactions. Frequently, these catalysts contain transition metal sites such as copper(I)[20] or zinc(II)[19] but lots of them are also based on iron(II) as the active species.[9,21] For hydrosilylation reactions several mechanisms were postulated, which differ in catalyst-substrate interaction. *Gade* et al. and *Huang* et al. published mechanisms for catalyzed iron(II) reactions with a direct metal-substrate interaction.[21a,21b] In contrast, *Nikonov* et al. and *Corriu* et al. achieved good conversions without any kind of Lewis-acid by simply adding smaller amounts of bases. They postulate a hypervalente hydrosilicate as the active species.[22] *Leyssens* et al. and *Nolan* et al. combined the benefits of both in their mechanism postulated for a copper(I) catalyzed hydrosilylation of ketones, which was supported by both, theoretical and experimental studies.[23] *Gade* et al. in 2008 published chiral iron(II) *N*,*N*,*N*-pincer complexes that gave good to excellent enantiomeric excesses in the catalytic hydrosilylation of ketones.[24] They also investigated the mechanism of this reaction by detailed studies including kinetic and quantum chemical methods. Other groups followed this strategy of ligand design by developing structurally related *N*-donor ligands and applied them for ketone hydrosilylation.[25]

In previous studies we could show that triphenylphosphine ruthenium(II) complexes bearing *N*,*N*-diallyl-2,6-bis(pyrazol-3-yl)pyridine ligands are highly active catalysts for the transfer hydrogenation of ketones and aldehydes with either 2-propanol or ethanol as the hydrogen source.[11a,11b] In addition, we could demonstrate the catalytic activity of iron(II) 2,6-bis(pyrazol-3-yl)pyridine and 2-(pyrazol-3-yl)pyridine complexes in ethylene polymerization[26] and in the hydrosilylation of ketones and aldehydes.[9] In this paper we describe the synthesis of novel chiral *N*-functionalized C_2-symmetric (2,6-bis(pyrazol-3-yl)pyridine)iron(II) complexes based on (1*R*,4*R*)-(+)-camphor and their application as catalysts for the hydrosilylation of ketones.

Results and Discussion

The ligands that were applied in this study for coordination to iron(II) chloride are accessible in a few steps starting from diethyl-2,6-pyridinedicarbonate (Scheme 1).[11b] Treatment of diethyl-2,6-pyridinedicarbonate with (1*R*,4*R*)-(+)-camphor and NaH in thf gave intermediate **1** in 65 % yield after recrystallization, which consists, according to its ^{1}H and ^{13}C NMR spectra, of a mixture of tautomers. Cyclization of **1** by reacting it with hydrazine hydrate in refluxing ethanol led to the enantiomerically pure and C_2-symmetric 2,6-bis(pyrazol-3-yl)pyridine **2** in 91 % yield. According to its ^{1}H and ^{13}C NMR spectra, which show only one set of signals, the tautomerism of the N-H protons is either rapid with respect to the NMR timescale or the protons are mainly located at one nitrogen atom as shown in Scheme 1. Deprotonation of the N-H groups and treatment with activated alkyl halides gave the *N*-alkylated ligands **3a,b**. In contrast to compound **2**, the resonances of the *meta*-protons of the pyridine ring are found shifted to lower field compared to the *para*-protons, which is a strong hint for

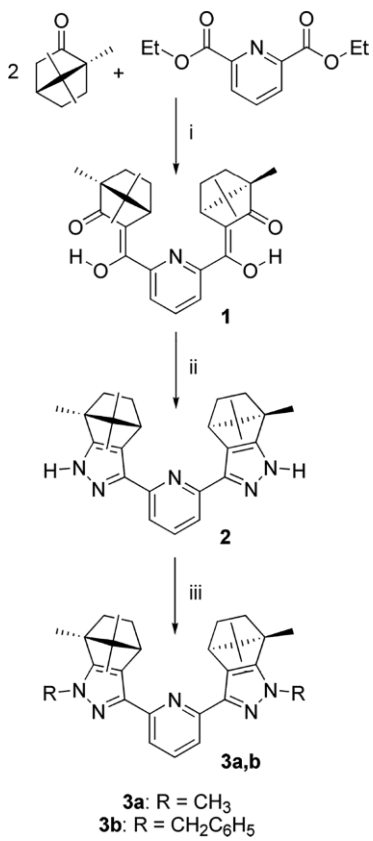

Scheme 1. Synthesis of the ligands **3a** and **3b**. (i) NaH, (1*R*,4*R*)-(+)-camphor, thf, 24 h, room temperature, diethyl-2,6-pyridinedicarbonate, 18 h, 60 °C; (ii) $N_2H_4{\cdot}H_2O$, EtOH, 4 h, refl.; (iii) **3a**: NaH, thf, 18 h, room temperature, $C_6H_5CH_2Br$, 24 h, refl., **3b**: $KN(SiMe_3)_2$, thf, 24 h, room temperature, CH_3I, 18 h, refl.

weak N···H–C interactions. In solution, compounds **3a,b** should therefore mainly occupy the conformation shown in Scheme 1.

Recrystallization of compounds **1**, **2** and **3a,b** resulted in the formation of colorless crystals, which were suitable for an X-ray structure analysis. The molecular structures of these compounds in the solid state are shown in Figures 1–3.

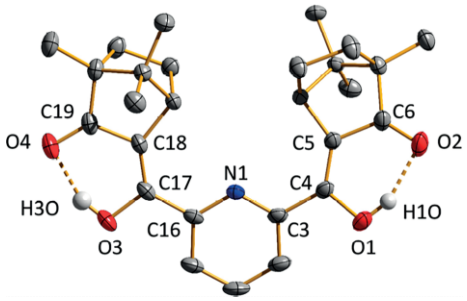

Figure 1. Molecular structure of compound **1** in the solid state. Carbon-bound hydrogen atoms are omitted for clarity. Characteristic bond lengths /Å, angles /° and dihedral angles /°: O1–C4 1.357(2), O2–C6 1.236(2), O3–C17 1.355(2), O4–C19 1.237(3), O1–H1O 0.88(3), O3–H3O 0.89(3), C4–C5 1.353(3), C5–C6 1.470(3), C17–C18 1.354(3), C18–C19 1.469(3), H1O···O2 1.78(3), H3O···O4 1.79(3), C4–O1–H1O 103(2), C17–O3–H3O 104(2), O2–C6–C5 126.50(17), C4–C5–C6 120.85(14), O3–C17–C18 120.36(19), C17–C18–C19 120.92(17), O1–H1O···O2 157(4), O3–H3O···O4 156(3), N1–C3–C4–O1–177.65(15), N1–C16–C17–O3 156.06(17).The ellipsoids are at the 50 % level.

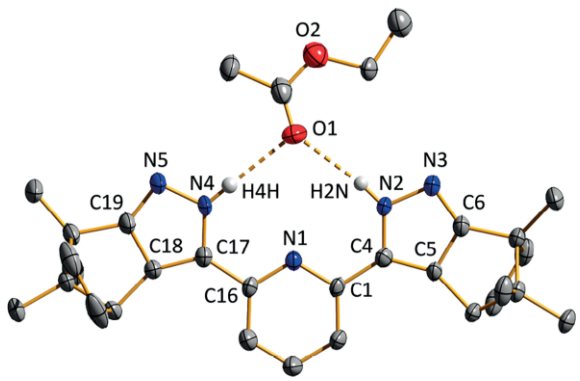

Figure 2. Molecular structure of compound **2** in the solid state. Carbon-bound hydrogen atoms are omitted for clarity. Characteristic bond lengths /Å, angles /° and dihedral angles /°: N2–H2N 0.86(3), N4–H4N 0.85(4), H2N···O1 2.23(4), H4N···O1 2.19(4), C4–N2–H2N 134(2), C17–N4–H4N 131(3), N2–H2NO1 170(4), N4–H4N···O1 179(7), N1–C1–C4–N2 3.1(5), N1–C16–C17–N4 0.1(5). The ellipsoids are at the 50 % level.

The tetraketone **1** crystallizes in the bis-enol form with the hydroxy groups being located at the pyridine-bound carbon atoms. The structural parameters are typical for 1,3-diketones in the ketoenol-form with alternating long (O1–C4, O3–C17, C5–C6, C18–C19) and short bonds (C4–C5, C6–O2, C17–C19, C19–O4) and typical hydrogen bond parameters of the O–H···O units.[27]

By recrystallization of the bispyrazolyl derivative **2** from ethyl acetate/*n*-hexane, one equivalent of the ester is found co-crystallized per molecule of **2** in the unit cell. For a perfect "chelating" hydrogen bond interaction, the NH units are located at the "inner" nitrogen atoms N2 and N4. This forces the pyrazole rings into an orientation almost coplanar to the central pyridine ring.

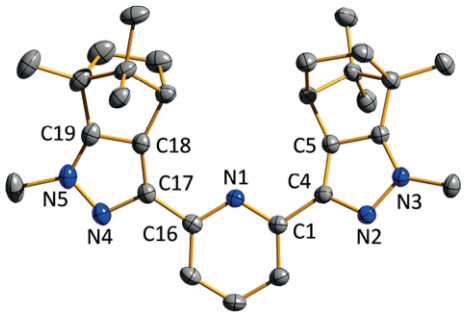

Figure 3. Molecular structure of compound **3a** in the solid state. Hydrogen atoms are omitted for clarity. Characteristic dihedral angles / °: N1–C1–C4–N2 170.30(15), N1–C16–C17–N4 160.27(15). The ellipsoids are at the 50 % level.

Due to weak interactions between the nitrogen atoms N2/N4 and the pyridine protons in the *meta*-position, compound **3a** adopts the typical all-*transoid* orientation of the pyrazolylpyridine fragments. A slight deviation from coplanarity of the pyrazole rings and the pyridine fragment is due to crystal packing effects. A similar solid-state structure was measured for compound **3b**. The according illustration and data can be found in the Supporting Information.

Reacting ligands **3a** and **3b** with equimolar amounts of $FeCl_2{\cdot}(H_2O)_4$ in dry methanol following a procedure from *Kuwata* and *Ikariya* led to the formation of the according dichlorido iron(II) complexes **4a** and **4b** in yields of approx. 70 % (Scheme 2).[28] In a similar reaction, ligand **3a** was treated with $Fe(OOCCH_3)_2$ in thf to produce the diacetato iron(II) complex **5a**.

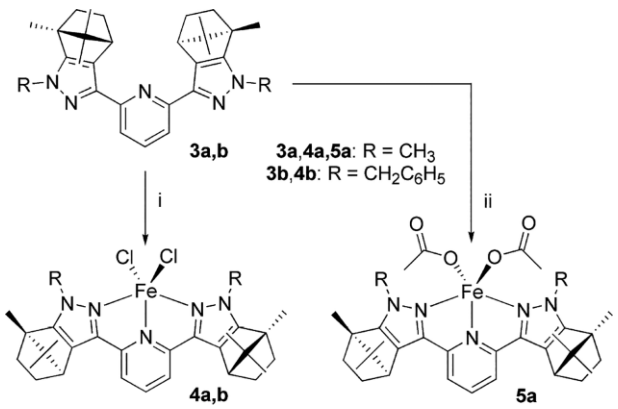

Scheme 2. Synthesis of the iron(II) complexes **4a**, **4b**, and **5a**. (i) $FeCl_2{\cdot}(H_2O)_4$, MeOH, 3 h, room temperature; (ii) $Fe(OOCCH_3)_2$, thf, 72 h, room temperature.

Crystals suitable for an X-ray structure analysis could be obtained from both dichlorido iron(II) complexes by slow diffusion of diethyl ether into saturated solutions of the compounds in dry methanol. The molecular structures of the iron(II) complexes **4a** and **4b** are shown in Figure 4.

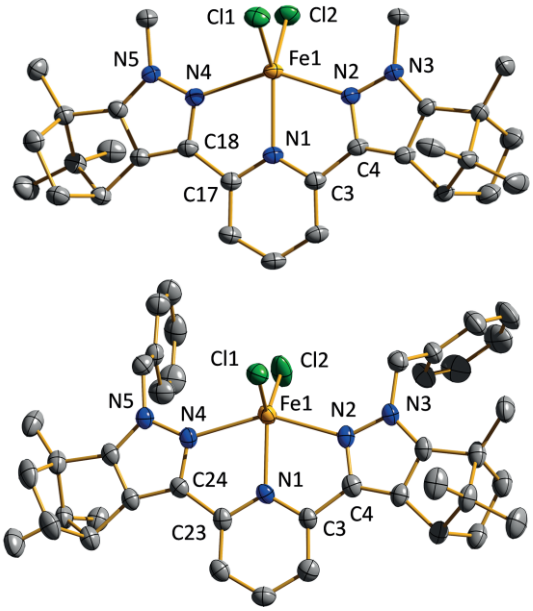

Figure 4. Molecular structures of compounds **4a** and **4b** in the solid state. Hydrogen atoms and solvent molecules (**4a**) are omitted for clarity. Characteristic bond lengths /Å, angles /° and dihedral angles /°: **4a** (top) Fe1–Cl1 2.3108(7), Fe1–Cl2 2.3380(8), Fe1–N1 2.187(2), Fe1–N2 2.206(2), Fe1–N4 2.200(2), Cl1–Fe1–Cl2 104.46(3), Cl1–Fe1–N1 129.67(6), Cl1–Fe1–N2 98.81(6), Cl1–Fe1–N4 104.41(6), Cl2–Fe1–N1 125.87(6), Cl2–Fe1–N2 102.25(6), Cl2–Fe1–N4 97.04(6), N1–Fe1–N2 72.29(8), N1–Fe1–N4 72.65(8), N2–Fe1–N4 144.91(8), N1–C3–C4–N2 –5.6(3), N1–C17–C18–N4 –6.0(3); **4b** (bottom) Fe1–Cl1 2.3103(14), Fe1–Cl2 2.2809(17), Fe1–N1 2.127(4), Fe1–N2 2.222(3), Fe1–N4 2.239(4), Cl1–Fe1–Cl2 121.53(6), Cl1–Fe1–N1 111.45(11), Cl1–Fe1–N2 93.10(10), Cl1–Fe1–N4 102.32(11), Cl2–Fe1–N1 126.91(11), Cl2–Fe1–N2 98.40(11), Cl2–Fe1–N4 96.72(11), N1–Fe1–N2 74.62(13), N1–Fe1–N4 74.10(13), N2–Fe1–N4 148.40(14), N1–C3–C4–N2 –6.4(7), N1–C23–C24–N4 –0.2(7). The ellipsoids are at the 50 % level.

The central iron(II) atoms in the complexes **4a** and **4b** are coordinated by three nitrogen atoms and two chlorido ligands in a distorted trigonal bipyramidal arrangement with the two chlorido ligands and the pyridine nitrogen atom occupying the equatorial positions. Overall, the structural parameters of the two complexes differ only marginally. Only the Fe1–N1 distance in **4b** is by 0.06 Å shorter than in **4a**, which can be explained by steric influence of the bulky benzyl groups on the $FeCl_2$ moiety. Due to structural restrictions of the tridentate *N*,*N*,*N*-donor, the N2–Fe–N4 angles (144.91°, 148.40°) deviate strongly from linearity. Compound **4a** crystallizes with one equivalent of methanol per formula unit which is bound to the chlorido ligand Cl2 by a weak hydrogen bond (not shown in Figure 4; distance H···Cl: 2.41 Å) in the solid state. This is in contrast to the findings of *Kuwata* and *Ikariya*,[26] who applied 2,6-bis(4-*tert*-butylpyrazol-3-yl)pyridine as the ligand for the synthesis of a dichlorido iron(II) complex. This ligand has intact N–H units and the resulting octahedral iron(II) complex coordinates methanol in the *trans*-position to the pyridine ligand. The difference in geometry can be explained by steric restrictions of the bulky alkyl substituents of the pyrazole nitrogen atoms in **4a** that would strongly interfere with an additional ligand in the *trans*-position to the pyridine ring. The Fe–Cl distances fit well with literature data of dichlorido iron(II) complexes bearing tridentate nitrogen ligands, such as terpyridine or 2,6-bis(dimethylamino)methylpyridine.[29] Single crystals of the acetato compound **5a** could not be obtained. However, elemental analysis, the infrared spectrum and the ^{57}Fe Mössbauer spectrum of this iron(II) complex strongly suggest a molecular structure similar to compounds **4a** and **4b**.

Some years ago, we reported a study on in-situ generated acetato and octanoato iron(II) compounds that catalyze the hydrosilylation of ketones.[9] Here we used 1-methyl-2-(pyrazol-3-yl)pyridine ligands, which we functionalized with electron donating and withdrawing substituents in the 4-position of the pyrazole to elucidate the electronic impact of these substituents on the activity of the catalysts. Since the dichlorido complexes **4a** and **4b** turned out not to be active in the hydrosilylation of ketones and since we found for the 1-methyl-2-(pyrazol-3-yl)pyridines that there is no difference in activity between the in-situ prepared and the isolated acetate complexes, we used the in-situ generation of the catalysts from iron(II) acetate and the chiral ligands **3a** and **3b** to evaluate the catalytic activity and in particular the stereoselectivity of these systems with acetophenone as the substrate and $HMeSi(OEt)_2$ as the silylating agent (Scheme 3).

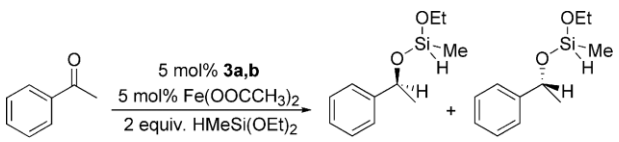

Scheme 3. Iron(II) catalysed hydrosilylation of acetophenone with ligands **3a** and **3b** (products after hydrolysis).

The in-situ complex formation was performed by reacting the ligand and iron(II) acetate in refluxing thf for 1 min. This procedure was applied to break up the polymeric structure of iron(II) acetate.[30] Then the silylating agent and acetophenone were added in one portion. Used ligands and related yields are shown in Table 1.

Table 1. Hydrosilylation of acetophenone catalysed by iron(II) complexes, in-situ formed from ligands **3a** and **3b** and $Fe(OOCCH_3)_2$.[a)]

Ligand	Yield / % [b)]		
	Acetophenone	Silyl ether [c)]	1-Phenylethanol
3a	1	90	9
3b	0	84	16

a) Reaction conditions: 1 mmol of acetophenone, 2 mmol of $HMeSi(OEt)_2$, 5 mol-% of $Fe(OOCCH_3)_2$, 5 mol-% of ligand, 3 mL of thf, 24 h, 65 °C. b) Uncorrected GC yields. c) Including mono- and polysilylethers.

Due to the excess of $HMeSi(OEt)_2$ used, the desired silyl ether shown in Scheme 3 and oxygen bridged polysilyl ethers were found as products as well as small amounts of 1-phenylethanol resulting from hydrolysis. The conversion of acetophenone is almost quantitative, however no excess of any of the two enantiomers could be observed under these conditions. To determine the enantiomeric excess, we followed a procedure published in the literature[19] to hydrolyse all the silyl ethers to

Table 2. Hydrosilylation of acetophenone with in-situ formed catalysts using ligands **3a** and **3b** and metal carboxylates at room temperature.[a].

Metal precursor	Ligand	Yield / % [b] Acetophenone	Silyl ether [c]	1-Phenylethanol
$Fe(OOCCH_3)_2$	**3a**	1	86	13
$Fe(OOCCH_3)_2$	**3b**	13	73	14
$Fe(OOCC_7H_{15})_2$	**3a**	0	100	0
$Co(OOCCH_3)_2{\cdot}(H_2O)_4$	**3a**	24	70	6
$Zn(OOCCH_3)_2{\cdot}(H_2O)_2$	**3a**	0	90	10
$Zn(OOCCH_3)_2$	**3a**	1	97	2

a) Reaction conditions: 1 mmol of acetophenone, 2 mmol of $HMeSi(OEt)_2$, 5 mol-% of metal precursor, 5 mol-% of ligand, 3 mL of thf, 24 h, room temperature. b) Uncorrected GC yields. c) Including mono- and polysilylethers.

Table 3. Hydrosilylation of acetophenone with complex **4a** and different bases at room temperature.[a].

Base	Reaction time / h	Yield / % [b] Acetophenone	Silyl ether	Polysilyl ether	1-Phenylethanol
None	24	100	0	0	0
$KOOCCH_3$	4.5	35	46	5	14
$KOOCCH_3$	6	26	53	13	18
KO*t*Bu	1	7	19	52	22
KO*t*Bu	6	7	25	60	8
NaOEtPh	0.5	1	47	45	7
NaOEtPh	1	1	45	50	4

a) Reaction conditions: 1 mmol of acetophenone, 2 mmol of $HMeSi(OEt)_2$, 10 mol-% of the base, 5 mol-% of **4a**, 3 mL of thf, room temperature. b) Uncorrected GC yields.

1-phenylethanol. After isolation, 1-phenylethanol was reacted, following a procedure published by *Hartung* et al.,[31] with 2-chloro-(4*R*,5*R*)-bis[(1*R*,2*S*,5*R*)-menth-1-yloxycarbonyl)]-1,3,2-dioxaphospholane to determine the enantiomeric excess of the alcohol by integration of the ^{31}P NMR signals of the two diastereomeric products.

In the following series of experiments we reduced the reaction temperature to 25 °C, hoping to find any stereoselective product formation. Since cobalt(II) and zinc(II) complexes had also shown their efficiency in asymmetric hydrosilylation reactions,[19,32,33] we also included cobalt(II) and zinc(II) acetate in our investigations. In addition, highly soluble iron(II) octanoate was used. The results are summarized in Table 2.

Interestingly, there are significant differences between various nitrogen donors and carboxylate ligands as well as between various metal sites which become apparent at room temperature. First, it looks like the bulky benzyl substituents at ligand **3b** lower the catalytic activity. The octanoato ligand in combination with the sterically less demanding ligand **3a** gave quantitative conversion and selectivity. The excellent conversion may be explained by the better solubility in thf of iron(II) octanoate compared to acetate. The outstanding selectivity towards the silyl ethers comes from the hydrophobic nature of the octanoate that impedes hydrolysis of the O–Si bond. In addition, zinc(II) acetate performs better in terms of selectivity than iron(II) acetate, which might be assigned to the higher Lewis-acidity of the iron(II) site. The presence of water from cobalt(II) and zinc(II) acetate hydrates leads to lower selectivities according to an increase of O–Si bond hydrolysis. For a stereoselective hydrosilylation of acetophenone, we tested ligand **3a** in combination with iron(II) acetate and found an enantiomeric excess of 12 % of 1(*S*)-phenylethanol (see Supporting Information).

Since we observed that only basic salts and complexes achieved good conversions in hydrosilylation reactions, we investigated complex **4a** in combination with different bases. To generate the catalyst in-situ, **4a** was reacted with the base in thf for 10 min before the addition of acetophenone and diethoxymethylsilane. The results are summarized in Table 3.

As already mentioned, complex **4a** is completely inactive in the absence of a base. However, with strong bases such as potassium *tert*-butanolate and sodium 1-phenylethanolate, rather high conversions could be obtained after short reaction times. The poor stereoselectivity we found for ligand **3a** in combination with iron(II) acetate can therefore be explained at least in parts by a parallel reaction of free acetate with the silylating agent.

Furthermore, we investigated the catalytic activity of the in-situ generated catalysts in the presence of the cheaper poly(methylhydrosiloxane) (Table 4). At room temperature only little conversion of acetophenone could be observed, however, raising the temperature to 65 °C gave almost quantitative conversion.

To follow the fate of the iron(II) catalyst during the hydrosilylation reaction, Mössbauer spectroscopy was applied. For this, complex **5a** was prepared with $^{57}Fe(OOCCH_3)_2$. Figure 5 shows the Mössbauer spectrum of ^{57}**5a** in the solid state exhibiting an isomer shift of $\delta = 1.24$ mm·s^{-1} and a quadrupole splitting of $\Delta E_Q = 3.02$ mm·s^{-1}. These values are comparable to those recorded for a five-coordinate dichloridoiron(II)terpyridine complex.[34]

During the catalytic hydrosilylation of acetophenone at room temperature with $HMeSi(OEt)_2$ as the hydrogen source and ^{57}**5a** as the catalyst liquid samples were taken after reaction times of 2, 4, 6, 24 and 48 h and immediately cooled to liquid nitrogen temperature ($T = 77$ K) in order to stop any

Table 4. Conversion of acetophenone to silyl ether with poly(methylhydrosiloxane) and different catalysts.[a].

Metal precursor	Solvent	Temperature / °C	Time / h	Conversion / %
$Fe(OOCCH_3)_2$	toluene	65	24	100
$Fe(OOCCH_3)_2$	toluene	room temperature	24	0
$Fe(OOCC_7H_{15})_2$	*n*-heptane	65	4	99
$Fe(OOCC_7H_{15})_2$	*n*-heptane	room temperature	24	24

a) Reaction conditions: 1 mmol of acetophenone, 2 mmol of poly(hydroxymethylsiloxane), 5 mol-% of metal precursor, 5 mol-% of ligand **3a**, 3 mL of solvent.

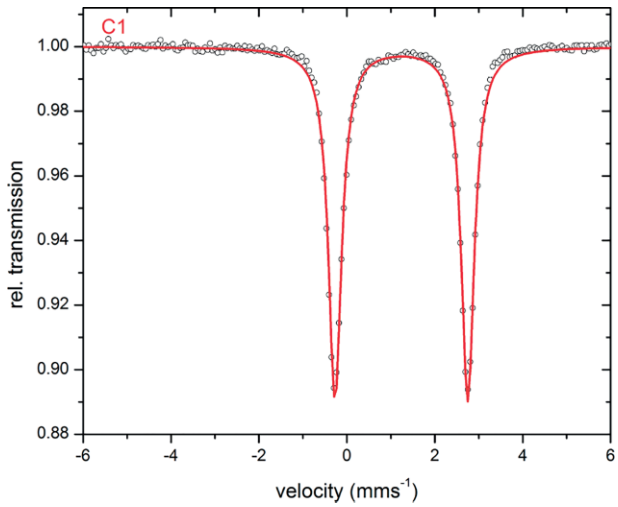

Figure 5. Mössbauer spectrum of compound ^{57}**5a** (C1) recorded at 77 K. The solid line is the result of a least square analysis with parameters given in Table SI1 (Supporting Information).

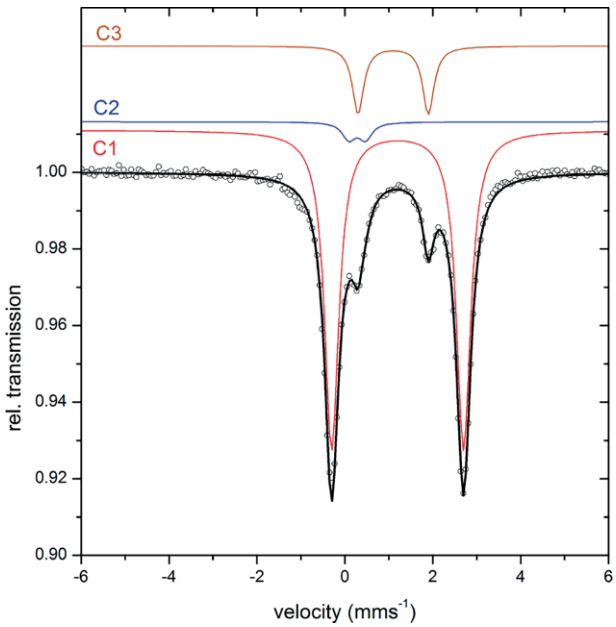

Figure 6. Mössbauer spectrum of the frozen catalysis solution obtained after a reaction time of 24 h (recorded at 77 K). The black line is the sum of the three components C1 (red), C2 (blue) and C3 (brown) obtained by a least square analysis with parameters given in Table SI1 (Supporting Information).

reactions. The according Mössbauer spectra can be found in the Supporting Information. After 2 h of reaction no changes in the Mössbauer spectrum could be detected. However, 4 h of reaction time led to the formation of a new component (C2) having an isomer shift of δ = 0.28 mm·s^{-1} and a quadrupole splitting of ΔE_Q = 0.38 mm·s^{-1}. These parameters are comparable to those measured for an iron(III) high-spin species coordinated by a terpyridine and three chlorido ligands.[35] The formation of a further component (C3) was detected in the Mössbauer spectrum after a reaction time of 6 h. The Mössbauer parameters of C3 (δ = 1.10 mm·s^{-1} and ΔE_Q = 1.60 mm·s^{-1}) are indicative for an iron(II) high-spin species.[36]

The Mössbauer spectrum obtained after a reaction time of 24 h is shown in Figure 6. In this spectrum, the same components as in the spectrum obtained after 6 h could be detected, but there is an increase in the relative contribution of the iron(II) high-spin species C3 from 1 % to 14 %. The iron(III) high-spin component C2 remains at approx. 4 %. At this point, the conversion of the substrate acetophenone is at 99 %. The Mössbauer spectrum proves that the active iron(II) catalyst C1 is still present in considerable amounts (82 %)

After 24 h an additional aliquot of substrates was added to the reaction mixture and the mixture was allowed to react for another 24 h. The according Mössbauer spectrum obtained from the mixture after a reaction time of overall 48 h again consists of the same three components (C1, C2, C3). However, the relative ratio of the components has changed (see Figure SMoss5, Supporting Information): The contribution of the iron (II) high-spin species (C3) has increased from 14 % to 25 % and that of the oxidized species (C2) has increased from 4 % to 16 %. The question is what type of iron(II) high-spin species (C3) has been formed during the catalysis. In principle a whole bunch of structurally different iron(II) complexes can be formed during the transformation. To get more information on C3, we synthesized as one possible candidate an iron(II) complex having two phenylethanolato ligands instead of the two acetato ligands of complex **5a**. The complex was barely stable, therefore no further analytic data was measured. Based on its Mössbauer spectrum, we can exclude that this complex is the unknown iron(II) high-spin component C3 (see Figure SMoss6, Supporting Information). We are presently looking for other candidates.

Conclusions

In this study, two chiral C_2-symmetric tridentate 2,6-bis(pyrazol-3-yl)pyridine ligands and a series of iron(II) complexes bearing these ligands were synthesized and spectroscopically

as well as structurally characterized. In comparison to previously studied iron(II) carboxylate complexes with bidentate *N*,*N*-donors, the novel, in-situ generated iron(II) carboxylate complexes allow to achieve excellent conversion of acetophenone in catalytic hydrosilylation reactions even at room temperature. However, the obtained enantiomeric excess of the resulting 1-phenylethanol is still poor. To get a deeper insight into the composition of the iron complexes in the reaction mixture, ^{57}Fe-Mössbauer spectra were recorded. According to our results, the in-situ formed carboxylate complexes are unambiguously involved in the catalytic reaction. However, a base is still requested to achieve significant conversions. This finding is in agreement with results of *Leyssens* et al. who postulate the cooperation of a base induced hypervalent hydrosilicate species and transition metal complexes as the active catalysts.[23a–23c]

Experimental Section

General Procedures: Chemicals were obtained from commercial suppliers and used without further purification. Air or moisture sensitive reactions were performed in dry glassware in an inert gas atmosphere (nitrogen). Methanol was dried with magnesium and distilled under nitrogen prior to use. Tetrahydrofuran was dried with sodium with benzophenone for indication and distilled under an inert atmosphere. Other solvents used were dried and purified by a MBraun MB-SPS-800 drying system. ATR-IR spectra were recorded with a Perkin–Elmer Spectrum 100 FT-IR spectrometer. NMR spectra were obtained with Bruker FT-NMR spectrometers AMX400 at 400.1 MHz (^{1}H) and 100.6 MHz (^{13}C) and AMX600 at 600 MHz (^{1}H) and 151 MHz (^{13}C) at room temperature. Chemical shifts δ (ppm) are reported with respect to residual solvent signals as internal standards. The assignment of the NMR resonances is according to the schemes given in the Supporting Information. High-resolution ESI$^+$ mass spectra and elemental analyses were performed by the analytical laboratory of the Fachbereich Chemie at the TU of Kaiserslautern. ^{57}Fe Mössbauer spectra were obtained in transmission geometry using a constant acceleration spectrometer operated in conjunction with a 512-channel analyzer (WissEl GmbH). The source contained ^{57}Co diffused in Rh with an activity of 1.4 GBq. The spectrometer was calibrated against α-iron at room temperature. A continuous flow cryostat (OptistatDN, Oxford Instruments) was used for variable temperature measurements. For further analysis, spectroscopic data were transferred from the multi-channel analyzer to a PC employing the public domain program Vinda running on an Excel 2003® platform.[37] The spectra were analyzed by least-squares fits using Lorentzian line shapes. In addition to the Mössbauer parameters isomer shift δ and quadrupole splitting ΔE_Q, the line width at half maximum Γ was determined.

2,6-Bis[(2-oxo-(1*R*,4*R*)-1,7,7-trimethylbicyclo[2.2.1]heptanyl)carbonyl]pyridine (1): 2.54 g (106 mmol) of NaH was suspended in a solution of 16.5 g (106 mmol) of (1*R*)-(+)-camphor in 180 mL of dry thf. The resulting reaction mixture was stirred for 24 h at room temperature and then heated to 60 °C. 5.92 g (26.5 mmol) of diethyl 2,6-pyridinedicarboxylate[11b] were added in small portions and the mixture was heated to reflux for 18 h. The resulting orange suspension was evaporated to dryness and the red-brown residue was dissolved by addition of 50 mL of 1 M KOH and 400 mL water. The basic aqueous phase was washed twice with 30 mL of CH_2Cl_2. The aqueous phase was treated with acetic acid until pH = 4 and extracted three times with 100 mL of CH_2Cl_2. After combination, the CH_2Cl_2 solutions were dried with $MgSO_4$ and the solvent was removed under reduced pressure to leave yellow, highly viscous foam. The raw product was crystallized from ethyl acetate/*n*-hexane to give colorless crystals. Yield: 7.57 g (65 %). $C_{27}H_{33}NO_4$ (387.57): calcd. C 74.45, H 7.64, N 3.22 %; found C 74.49, H 7.62, N 3.11 %. M. p.: 122.6 °C. The ^{1}H and ^{13}C NMR spectra show a multitude of resonances due to ketoenol tautomerism, which cannot be completely assigned. **^{1}H NMR** (400.1 MHz, $CDCl_3$): δ = 12.59–12.26 (m, 1 H, H15), 8.25–8.01 (m, 2 H, H2), 7.95 (t, $^3J_{HH}$ = 8.0 Hz, 1 H, H1), 4.85–4.83 (m, 1 H, H5), 3.74–3.61 (m, 1 H, H10), 2.65–2.58 (m, 1 H, H10), 2.12–2.08 (m, 1 H, H9), 1.77–1.69 (m, 4 H, H9, H8), 1.53–1.48 (m, 2 H, H8), 1.37–1.32 (m, 1 H, H9), 1.06–1.02 (m, 7 H, H14, H11), 0.98 (s, 6 H, H13), 0.85–0.80 (m, 5 H, H11). **^{13}C NMR** (100.6 MHz, $CDCl_3$): δ = 215.5, 215.3, 210.6, 199.1, 198.2, 196.0, 158.0, 157.4, 157.2, 139.1, 137.6, 127.0, 123.2, 118.2, 117.9, 117.6, 62.5, 59.5, 59.5, 58.7, 58.5, 58.4, 58.2, 58.0, 49.8, 49.6, 48.9, 48.72, 48.66, 48.5, 48.0, 47.2, 46.8, 45.4, 31.4, 31.3, 31.0, 30.4, 29.6, 29.5, 29.1, 28.0, 27.2, 27.1, 23.1, 22.8, 22.7, 22.0, 21.3, 21.0, 20.9, 20.6, 20.3, 19.6, 19.4, 19.3, 19.2, 19.2, 14.5, 10.1, 10.1, 9.3, 9.2. **IR** (ATR): $\tilde{\nu}$ = 2959m, 2872w, 1675s, 1620m (2 × νC=O), 1567s, 1439m, 1390m, 1374m, 1340s, 1288s, 1172w, 1134w, 1108m, 1069vs, 1029vs, 990m, 817vs, 791s, 739s, 667m cm^{-1}. **HR-GC-MS** ($C_{27}H_{33}NO_4$): *m*/*z* calcd. 435.2410; found 435.2422.

2,6-Bis((1*R*,4*R*)-1,7,7-trimethylbicyclo[2.2.1]heptanylpyrazol-3-yl) pyridine (2): 2.18 g (5.00 mmol) of compound **1** were dissolved in 30 mL of ethanol. 2.58 mL (65.0 mmol) of hydrazine hydrate were added and the reaction mixture was heated to reflux for 4 h. The yellow solution was evaporated to dryness, the remaining beige residue was dissolved in 30 mL of ethyl acetate (30 mL) and the resulting solution was washed four times with 15 mL of water. After drying the organic phase with $MgSO_4$ the solvent was removed under reduced pressure to leave a colorless solid. The raw product was recrystallized from ethyl acetate/*n*-hexane to give colorless crystals. Yield 1.95 g (91 %). $C_{27}H_{33}N_5$ (427.59): calcd. C 75.84, H 7.78, N 16.38 %; found C 75.33, H 7.71, N 16.15 %. **^{1}H NMR** (400.1 MHz, $CDCl_3$): δ = 7.73 (t, $^3J_{HH}$ = 8.0 Hz, 1 H, H3), 7.41 (d, $^3J_{HH}$ = 8.0 Hz, 2 H, H2), 3.06 (d, $^3J_{HH}$ = 4.0 Hz, 2 H, H10), 2.20–2.13 (m, 2 H, H9$_{eq}$), 1.93–1.86 (m, 2 H, H8$_{eq}$), 1.40–1.37 (m, 2 H, H8$_{ax}$), 1.33 (s, 6 H, H11), 1.30–1.23 (m, 2 H, H9$_{ax}$), 1.00 (s, 6 H, H13), 0.73 (s, 6 H, H14). **^{13}C NMR** (100.6 MHz, $CDCl_3$): δ = 167.7 (C1), 148.6 (C3), 138.1 (C2), 134.4 (C4), 125.56 (C6), 119.5 (C5), 61.9 (C12), 51.0 (C7), 48.6 (C10), 33.9 (C8), 27.6 (C9), 21.0 (C14), 19.7 (C13), 11.0 (C11). **IR** (ATR): $\tilde{\nu}$ = 3347m, 3188m, 2949s, 2869m, 1614w, 1585m, 1567vs, 1491vs, 1475m, 1454m, 1415s, 1385m, 1365w, 1338w, 1300w, 1289m, 1271m, 1238m, 1151m, 1100m, 1077m, 1054w, 1021w, 993s, 980s, 959w, 909w, 878w, 833w, 810s, 787s, 730m, 709m cm^{-1}. **HR-GC-MS** ($C_{27}H_{33}N_5$): *m*/*z* calcd. 427.2736; found 427.2752.

2,6-Bis(*N*-methyl-(1*R*,4*R*)-1,7,7-trimethylbicyclo[2.2.1]heptanyl-pyrazol-3-yl)pyridine (3a): 724 mg (3.45 mmol) of $KN(SiMe_3)_2$ were suspended in 20 mL of dry thf. 737 mg (1.72 mmol) of compound **2** were added and the reaction mixture was stirred for 24 h at room temp. During this time, the color of the mixture and changed to dark red. Then any volatiles were removed under reduced pressure and another 20 mL of dry thf were added. 494 mg (3.45 mmol) of CH_3I were added and the mixture was heated to reflux for 18 h. The solvent was removed under reduced pressure, the solid residue was treated with 20 mL of CH_2Cl_2, the resulting yellow suspension was washed twice with 35 mL of water, dried with $MgSO_4$ and the solvent was again removed under reduced pressure leaving a colorless solid. The raw product was recrystallized from ethyl acetate/*n*-hexane to give colorless crystals. Yield: 550 mg (70 %). $C_{33}H_{43}N_5$ (508.67): calcd. C 76.44, H 8.18, N 15.37; found C 76.14, H 8.15, N 15.17 %. **^{1}H NMR**

(400.1 MHz, $CDCl_3$): δ = 7.71 (d, $^3J_{HH}$ = 8.0 Hz, 2 H, H2), 7.64 (dd, $^3J_{HH}$ = 8.0, $^3J_{HH}$ = 8.0 Hz, 1 H, H1), 3.89 (s, 6 H, H15), 3.28 (d, $^3J_{HH}$ = 4.0 Hz, 2 H, H10), 2.13–2.08 (m, 2 H, $H9_{eq}$), 1.85–1.82 (m, 2 H, $H8_{eq}$), 1.37 (s, 6 H, H11), 1.33–1.27 (m, 4 H, $H8_{ax}$, $H9_{ax}$), 0.94 (s, 6 H, H14), 0.80 (s, 6 H, H13). **^{13}C NMR** (100.6 MHz, $CDCl_3$): δ = 155.5 (C1), 152.7 (C4), 143.9 (C6), 136.8 (C3), 128.3 (C5), 118.1 (C2), 62.7 (C7), 52.7 (C12), 48.8 (C10), 37.3 (C15), 33.8 (C8), 27.5 (C9), 20.6 (C14), 19.8 (C13), 11.4 (C11). **IR** (ATR): $\tilde{\nu}$ = 2979m, 2952m, 2870m, 1599w, 1571vs, 1529m, 1472w, 1455m, 1428s, 1409m, 1387m, 1222w, 1147w, 1131w, 1106m, 1056w, 1019m, 1001w, 930w, 919w, 827vs, 822vs, 778w, 750m, 724w, 691w, 662m cm^{-1}. **HR-GC-MS** ($C_{29}H_{37}N_5$): *m/z* calcd. 455.3049; found: 455.3062.

2,6-Bis(*N*-benzyl-(1*R*,4*R*)-1,7,7-trimethylbicyclo[2.2.1]heptanyl-pyrazol-3-yl)pyridine (3b): 240 mg (10 mmol) of NaH were suspended in 50 mL of dry thf. 1.71 g (4.00 mmol) of compound **2** were added and the reaction mixture was stirred for 18 h at room temp. During this time the color of the mixture changed to dark red. 1.75 g (10 mmol) of benzylic bromide were added and the mixture was heated to reflux for 24 h. Then the solvent was removed and the residue was treated with 30 mL of CH_2Cl_2. The mixture was washed twice with 15 mL of water and the organic phase was dried with $MgSO_4$. Removal of the solvent resulted in a yellow, highly viscous foam. The raw product was recrystallized from *n*-hexane to give colorless crystals. Yield: 1.74 g (71 %). $C_{41}H_{47}N_5 \cdot (C_6H_{14})_{0.5}$ (625.95): calcd. C 80.94, H 8.34, N 10.73 %; found C 81.02, H 7.90, N 10.54 %. **^{1}H NMR** (400.1 MHz, $CDCl_3$): δ = 7.84 (d, $^3J_{HH}$ = 8.0 Hz, 2 H, H2), 7.68 (t, $^3J_{HH}$ = 8.0 Hz, 1 H, H1), 7.30–7.11 (m, 10 H, H17, H18, H19), 5.42 (d, $^2J_{HH}$ = 16.0 Hz, 2 H, H15), 5.33 (d, $^2J_{HH}$ = 16.0 Hz, 2 H, H15), 3.32 (d, $^3J_{HH}$ = 4.0 Hz, 2 H, H10), 2.11–2.02 (m, 2 H, $H9_{eq}$), 1.72–1.68 (m, 2 H, $H8_{eq}$), 1.38–1.32 (m, 2 H, $H8_{ax}$), 1.16 (s, 6 H, H11), 1.12–1.05 (m, 2 H, $H9_{ax}$), 0.88 (s, 6 H, H14), 0.77 (s, 6 H, H13). **^{13}C NMR** (100.6 MHz, $CDCl_3$): δ = 155.3 (C3), 152.9 (C4), 144.3 (C6), 138.2 (C16), 136.8 (C1), 129.2 (C5), 128.7 (C19), 127.6 (C17), 126.7 (C18), 118.3 (C2), 62.9 (C7), 54.3 (C15), 52.8 (C12), 48.9 (C10), 33.5 (C8), 27.5 (C9), 20.6 (C14), 19.8 (C13), 11.4 (C11) ppm. **IR** (ATR): $\tilde{\nu}$ = 3056w, 2955s, 2870m, 1597w, 1569vs, 1539w, 1524m, 1497m, 1420vs, 1387m, 1365w, 1312w, 1285m, 1272m, 1254w, 1189w, 1178w, 1148w, 1120m, 1088s, 1077s, 1060m, 1030w, 1004m, 928w, 859w, 842w, 832w, 821vs, 746s, 727s, 701vs, 663s cm^{-1}.

General Procedure for the Synthesis of the Dichloride Iron(II) Complexes: $FeCl_2 \cdot (H_2O)_4$ was dissolved in 5 mL of dry MeOH and ligand **3a** resp. **3b** was added whilst stirring. The color of the solution turned immediately to orange-red. The reacting mixture was stirred for 3 h at room temp. Then the volume of the solvent was reduced to 2 mL and 25 mL of dry diethyl ether were added slowly to precipitate the product. The received red solids were recrystallized from dry MeOH/diethyl ether.

[2,6-Bis(*N*-methyl-(1*R*,4*R*)-1,7,7-trimethylbicyclo[2.2.1]heptanyl-pyrazol-3-yl)pyridine]dichloridoiron(II) (4a): Synthesized from 57.7 mg (0.29 mmol) of $FeCl_2 \cdot (H_2O)_4$ and 151 mg (0.33 mmol) of **3a**. Yield 120 mg (71 %). $C_{29}H_{37}Cl_2FeN_5 \cdot CH_3OH$: calcd. C 58.64, H 6.73, N 11.40 %; found C 58.76, H 6.74, N 10.97 %. **IR** (ATR): $\tilde{\nu}$ = 2959w, 2876w, 1604w, 1572w, 1550w, 1451s, 1413w, 1351m, 1303w, 1286m, 1271w, 1248w, 1155m, 1122m, 1051w, 841w, 819s, 779w, 746m, 691w, 662w cm^{-1}.

[2,6-bis(*N*-benzyl-(1*R*,4*R*)-1,7,7-trimethylbicyclo[2.2.1]heptanyl-pyrazol-3-yl)pyridine]dichloridoiron(II) (4b): Synthesized from 67.6 mg (0.349 mmol) of $FeCl_2 \cdot (H_2O)_4$ and 207 mg (0.34 mmol) of ligand **3b**. Yield: 175 mg (70 %). $C_{41}H_{45}Cl_2FeN_5$: calcd. C 67.04, H 6.17, N 9.53 %; found C 66.74, H 6.21, N 9.48 %. **IR** (ATR): $\tilde{\nu}$ = 3009w, 2958m, 2875w, 1603m, 1575m, 1497m, 1452s, 1391w, 1346m, 1318w, 1290w, 1271w, 1251w, 1227w, 1206w, 1163m, 1125vs, 1075m, 1054m, 1029w, 1015w, 919w, 827w, 814s, 780w, 765w, 734vs, 723s, 701s, 692s, 669m cm^{-1}.

[2,6-Bis(*N*-methyl-(1*R*,4*R*)-1,7,7-trimethylbicyclo[2.2.1]heptanyl-pyrazol-3-yl)pyridine]diacetatoiron(II) (5a): 62.3 mg (0.36 mmol) of colorless iron(II) acetate were dissolved in 12 mL of dry thf and 179 mg of (0.39 mmol) of ligand **3a** were added. The pale yellow reaction mixture was stirred for 72 h at room temperature, while it transformed into an deep red solution. Afterwards the solvent was removed under reduced pressure, the dark red solid was washed twice with 5 mL of degassed *n*-pentane and dried under reduced pressure. Yield: 150 mg (67 %). $C_{33}H_{43}FeN_5O_4$: calcd. C 62.96, H 6.88, N 11.12 %; found C 62.59, H 7.15, N 11.17 %. **IR** (ATR): $\tilde{\nu}$ = 2953m, 2869w, 1570vs, 1452vs, 1429vs, 1413vs, 1388vs, 1376vs, 1367vs, 1314m, 1271s, 1247m, 1156m, 1125m, 1047m, 1011m, 931w, 921w, 819s, 778w, 743m, 675w cm^{-1}. **ESI-MS**: *m/z* calcd. for $[M\text{-}OOCCH^3]^+$ 570.25, found: 570.00.

Catalytic Reactions: All catalytic experiments were performed in crimp top vials purchased from VWR International GmbH with a total volume of 20 mL. Acetophenone, catalysts and bases were weighed and filled in the vials, a magnetic stirring bar was added and the vials were sealed with ptfe septa. Fluid components and substrates were added by Hamilton® syringes. The vials were placed in a preheated aluminum heating block with normed boreholes. Samples of 0.1 mL were taken with single use syringes and cannula (Braun GmbH). The samples were filtered through a short column filled with small amounts of neutral aluminum oxide and $MgSO_4$ and eluted with ethyl acetate. The samples were analyzed using a Clarus 580 GC equipped with a FID-detector or a Varian 3900 GC-MS (2100T). GC columns: FS-OV-1701-CB-0.25 (30 m, d = 0.25 mm, CS Chromatographie Service GmbH). Helium (60 kPa) was used as the carrier gas. The injector temperature was set to 250 °C with a split-value of 25:8 and an oven temperature heating rate of 6 K·min^{-1} starting from 80 °C and ending after 30 min at 260 °C.

X-ray Structure Analysis: Crystal data and refinement parameters are collected in Table 5. All structures were solved by direct methods (SIR92[38] for **1**, **2**, **3a**, **3b** and **4a**, SIR2011[39] for **4b**), completed by subsequent difference Fourier syntheses, and refined by full-matrix least-squares procedures.[40] Semi-empirical absorption corrections from equivalents (Multiscan) were carried out for **1**, **2**, **3a** and **3b**, while analytical numeric absorption corrections were applied on complexes **4a** and **4b**.[41] All non-hydrogen atoms were refined with anisotropic displacement parameters. In the structure of compound **1** the hydrogen atoms which are bound to the oxygen atoms O1 and O3, were located in the difference Fourier synthesis, and were then refined freely. The hydrogen atoms, which are bound to the nitrogen atoms N2 and N4 in the structure of compound **2**, were located in the difference Fourier synthesis, and were refined semi-freely with the help of a distance restraint, while constraining their *U*-values to 1.2 times the *U*(eq) values of corresponding nitrogen atoms. All the other hydrogen atoms were placed in calculated positions and refined by using a riding model.

Crystallographic data (excluding structure factors) for the structures in this paper have been deposited with the Cambridge Crystallographic Data Centre, CCDC, 12 Union Road, Cambridge CB21EZ, UK. Copies of the data can be obtained free of charge on quoting the depository numbers CCDC-1968102, CCDC-1968103, CCDC-1968104, CCDC-1968105, CCDC-1968106, and CCDC-1968107 (Fax: +44-1223-336-033; E-Mail: deposit@ccdc.cam.ac.uk, http://www.ccdc.cam.ac.uk).

Table 5. Crystallographic data, data collection, and refinement.

	1	**2**	**3a**	**3b**	**4a**	**4b**
Empirical formula	$C_{27}H_{33}NO_4$	$C_{31}H_{41}N_5O_2$	$C_{29}H_{37}N_5$	$C_{47}H_{59}N_5$	$C_{30}H_{41}Cl_2FeN_5O$	$C_{41}H_{45}Cl_2FeN_5$
Formula weight	435.54	515.69	455.63	693.99	614.43	734.57
Crystal size / mm	0.628×0.432×0.241	0.571×0.417×0.349	0.403×0.397×0.321	0.426×0.395×0.280	0.520×0.170×0.130	0.39×0.27×0.19
T /K	150(2)	150(2)	150(2)	150(2)	150(2)	150(2)
λ /Å	0.71073	1.54184	1.54184	1.54184	1.54184	1.54184
Crystal system	monoclinic	monoclinic	orthorhombic	monoclinic	orthorhombic	monoclinic
Space group	$P2_1$	$P2_1$	$P2_12_12_1$	$C2$	$P2_12_12_1$	$P2_1$
a /Å	7.1868(2)	7.5020(1)	10.5733(1)	16.6302(2)	7.2604(1)	9.2391(2)
b /Å	16.4626(4)	11.3688(2)	10.9772(1)	22.5696(3)	19.0798(2)	13.1120(2)
c /Å	10.1309(2)	17.0710(3)	21.8900(2)	11.0605(1)	22.8949(3)	15.2307(3)
α /°	90	90	90	90	90	90
β /°	100.194(2)	101.494(2)	90	99.745(1)	90	94.992(2)
γ /°	90	90	90	90	90	90
V /Å^3	1179.70(5)	1426.77(4)	2540.67(4)	4091.54(8)	3171.56(7)	1838.09(6)
Z	2	2	4	4	4	2
$\rho_{calcd.}$ /g·cm^{-3}	1.226	1.200	1.191	1.127	1.287	1.327
μ /mm^{-1}	0.081	0.601	0.550	0.501	5.596	4.903
θ-range /°	2.880–32.263	4.703–62.591	4.039–62.664	3.332–62.702	3.861–62.731	4.457–62.622
Refl. coll.	13481	8624	18315	14921	11781	8299
Indep. refl.	7397 [R_{int} = 0.0216]	4260 [R_{int} = 0.0150]	4052 [R_{int} = 0.0207]	6162 [R_{int} = 0.0172]	5069 [R_{int} = 0.0264]	4646 [R_{int} = 0.0223]
Data / restr. / param.	7397/1/303	4260/3/357	4052/0/315	6162/37/479	5069/0/362	4646/1/448
Final R indices [$I > 2\sigma(I)$] [a]	0.0439, 0.1037	0.0499, 0.1389	0.0284, 0.0730	0.0378, 0.0973	0.0262, 0.0589	0.0501, 0.1310
R ind. (all data)	0.0492, 0.1071	0.0501, 0.1391	0.0287, 0.0732	0.0379, 0.0976	0.0277, 0.0595	0.0512, 0.1329
Absolute structure param.	–0.4(4)	–0.02(5)	–0.05(8)	–0.02(9)	–0.0022(18)	–0.008(5)
GooF [b]	1.029	1.064	1.048	1.053	1.038	1.044
$\Delta\rho_{max\ /min}$ / e·Å^{-3}	0.308/–0.156	0.657/–0.209	0.153/–0.159	0.229/–0.260	0.388/–0.215	0.657/–0.295

a) $R_1 = \Sigma||F_o| - |F_c||/\Sigma|F_o|$, $wR_2 = [\Sigma w(F_o^2 - F_c^2)^2/\Sigma wF_o^2]^{1/2}$. b) GooF = $[\Sigma w(F_o^2 - F_c^2)^2/(n - p)]^{1/2}$.

Supporting Information (see footnote on the first page of this article): The supporting information contains NMR and IR spectra of the compounds, data for the determination of the enantiomeric excess, the molecular structure of compound **3b** and additional Mössbauer data.ll as X-ray data.

Acknowledgements

The authors gratefully acknowledge financial support by the DFG priority program SFB/TRR 88 (3MET). Open access funding enabled and organized by Projekt DEAL.

Keywords: *N*-donor ligands; Iron; Catalysis; Hydrosilylation; Mössbauer spectroscopy

References

[1] a) P. T. Anastas, I. T. Horváth, *Chem. Rev.* **2007**, *107*, 2169–2173; b) M. A. Dubé, S. Salehpour, *Macromol. React. Eng.* **2014**, *8*, 7–8.
[2] a) C. Janiak, E. Riedel, *Moderne Anorganische Chemie*, deGruyter, Berlin, **2007**, pp. 725–756; b) A. Behr, *Angewandte homogene Katalyse*, Wiley-VCH, Weinheim, **2008**, pp. 3–79; c) G. Zassinovich, G. Mestroni, S. Gladiali, *Chem. Rev.* **1992**, *92*, 1051–1059; d) R. Noyori, *Angew. Chem. Int. Ed.* **2002**, *41*, 2008–2022; e) C. C. C. Johansson Seechurn, M. O. Kitching, T. J. Colacot, V. Snieckus, *Angew. Chem. Int. Ed.* **2012**, *51*, 5062–5085.
[3] D. Wang, D. Astruc, *Chem. Rev.* **2015**, *115*, 6621–6686.
[4] C. Bolm, J. Legros, J. LePaih, L. Zani, *Chem. Rev.* **2004**, *104*, 6217–6254.
[5] a) S. G. Shepard, S. M. Fatur, A. K. Rappé, N. H. Damrauer, *J. Am. Chem. Soc.* **2016**, *138*, 2949–2952; b) T. D. Roberts, M. A. Little, L. J. K. Cook, S. A. Barrett, F. Tuna, M. A. Halcrow, *Polyhedron* **2013**, *64*, 4–12.
[6] a) S. A. M. Smith, R. H. Morris, *Synthesis* **2015**, *47*, 1775–1779; b) A. A. Mikhailine, M. I. Maishan, A. J. Lough, R. H. Morris, *J. Am. Chem. Soc.* **2012**, *134*, 12266–12280.
[7] a) B. L. Small, M. Brookhart, A. M. A. Bennet, *J. Am. Chem. Soc.* **1998**, *120*, 4049–4050; b) B. L. Small, M. Brookhart, *J. Am. Chem. Soc.* **1998**, *120*, 7143–7144; c) B. L. Small, M. Brookhart, *Macromolecules* **1999**, *32*, 2120–2130; d) E. L. Dias, M. Brookhart, P. S. White, *Organometallics* **2000**, *19*, 4995–5004; e) G. J. P. Britovsek, V. C. Gibson, B. S. Kimberley, P. J. Maddox, S. J. McTavish, G. A. Solan, A. J. P. White, D. J. Williams, *Chem. Commun.* **1998**, 849–850; f) G. K. B. Glentsmith, V. C. Gibson, P. B. Hitcock, B. S. Kimberley, C. W. Rees, *Chem. Commun.* **2002**, 1498–1499; g) V. C. Gibson, K. P. Tellmann, M. J. Humphries, D. F. Wass, *Chem. Commun.* **2002**, 2316–2317.
[8] R. H. Morris, *Chem. Soc. Rev.* **2009**, *38*, 2282–2291.
[9] K. Müller, A. Schubert, T. Jozak, A. Ahrens-Botzong, V. Schünemann, W. R. Thiel, *ChemCatChem.* **2011**, *3*, 887–892.
[10] a) M. A. Yurovskaya, A. V. Karchava, *Chem. Heterocycl. Compd.* **1994**, *30*, 1331–1385; b) M. A. Yurovskaya, O. D. Mit'kin, F. V. Zaitseva, *Chem. Heterocycl. Compd.* **1998**, *34*, 871–899.

[11] a) L. Taghizadeh Ghoochany, S. Farsadpour, Y. Sun, W. R. Thiel, *Eur. J. Inorg. Chem.* **2011**, 3431–3437; b) P. Weingart, W. R. Thiel, *ChemCatChem.* **2018**, *10*, 4844–4848; c) C. Groß, Y. Sun, T. Jost, T. Grimm, M. Klein, G. Niedner-Schatteburg, S. Becker, W. R. Thiel, *Chem. Commun.* **2020**, *56*, 368–371.
[12] a) P. van der Valk, P. G. Potvin, *J. Org. Chem.* **1994**, *59*, 1766–1770; b) M. A. Halcrow, *Coord. Chem. Rev.* **2009**, *253*, 2493–2514; c) W. R. Thiel, J. Eppinger, *Chem. Eur. J.* **1997**, *3*, 696–705; d) H. Glas, M. Barz, W. R. Thiel, *J. Organomet. Chem.* **2001**, *621*, 153–157; e) A.-K. Pleier, H. Glas, M. Grosche, P. Sirsch, W. R. Thiel, *Synthesis* **2001**, 55–62.
[13] T. Inagaki, L. T. Phong, A. Furuta, J. Ito, H. Nishiyama, *Chem. Eur. J.* **2010**, *16*, 3090–3096.
[14] P. Liu, E. L. Wong, A. W. Yuen, C. Che, *Org. Lett.* **2008**, *10*, 3275–3278.
[15] a) J. K. Whitesell, *Chem. Rev.* **1989**, *89*, 1581–1590; b) A. Pfaltz, W. J. Drury III, *Proc. Natl. Acad. Sci. USA* **2004**, *101*, 5723–5726.
[16] A. A. Watson, D. A. House, P. J. Steel, *J. Org. Chem.* **1991**, *56*, 4072–4074.
[17] W. R. Thiel, M. Angstl, T. Priermeier, *Chem. Ber.* **1994**, *127*, 2373–2377.
[18] a) M. Jia, W. R. Thiel, *Chem. Commun.* **2002**, 2392–2393; b) M. Jia, A. Seifert, M. Berger, H. Giegengack, S. Schulze, W. R. Thiel, *Chem. Mater.* **2004**, *16*, 877–893.
[19] V. Surzhko, T. Roisnel, B. Le Grel, C. Lalli, G. Argouarch, *Tetrahedron Lett.* **2017**, *58*, 1343–1347.
[20] a) H. Ito, T. Ishizuka, T. Okumura, H. Yamanaka, J. Tateiwa, M. Sonoda, A. Hosomi, *J. Organomet. Chem.* **1999**, *574*, 102–106; b) B. H. Lipshutz, K. Noson, W. Chrisman, A. J. Lower, *J. Am. Chem. Soc.* **2003**, *125*, 8779–8789.
[21] a) Z. Zuo, L. Zhang, X. Leng, Z. Huang, *Chem. Commun.* **2015**, *51*, 5073–5076; b) S. P. Thomas, D. J. Frank, M. D. Greenhalgh, *Adv. Synth. Catal.* **2014**, *356*, 584–590.
[22] a) K. Revunova, G. I. Nikonov, *Chem. Eur. J.* **2014**, *20*, 839–845; b) C. Chuit, R. J. P. Corriu, C. Reye, J. C. Young, *Chem. Rev.* **1993**, *93*, 1371–1448.
[23] a) T. Vergote, T. Gathy, F. Nahra, O. Riant, D. Peeters, T. Leyssens, *Theor. Chem. Acc.* **2012**, *131*, 1–13; b) T. Vergote, S. Gharbi, F. Billard, O. Riant, T. Leyssens, *J. Organomet. Chem.* **2013**, *745–746*, 133–139; c) T. Vergote, F. Nahra, A. Merschaert, O. Riant, D. Peeters, T. Leyssens, *Organometallics* **2014**, *33*, 1953–1963; d) S. Díez-González, H. Kaur, F. K. Zinn, E. D. Stevens, S. P. Nolan, *J. Org. Chem.* **2005**, *70*, 4784–4796; e) S. Díez-González, S. P. Nolan, *Acc. Chem. Res.* **2008**, *41*, 349–358; f) S. Díez-González, S. P. Nolan, *Aldrichimica Acta* **2008**, *41*, 43–51.
[24] a) B. K. Langlotz, H. Wadepohl, L. H. Gade, *Angew. Chem. Int. Ed.* **2008**, *47*, 4670–4674; b) T. Bleith, L. H. Gade, *J. Am. Chem. Soc.* **2016**, *138*, 4972–4983; c) T. Bleith, H. Wadepohl, L. H. Gade, *J. Am. Chem. Soc.* **2015**, *137*, 2456–2459; d) D. Sauer, H. Wadepohl, L. H. Gade, *Inorg. Chem.* **2012**, *51*, 12948–12958.
[25] a) K. Kobayashi, Y. Izumori, D. Taguchi, H. Nakazawa, *ChemPlusChem.* **2019**, *84*, 1094–1102; b) Z. Zuo, L. Zhang, X. Leng, Z. Huang, *Chem. Commun.* **2015**, *51*, 5073–5076; c) T. Inagaki, A. Ito, J. Ito, H. Nishiyama, *Angew. Chem. Int. Ed.* **2010**, *49*, 9384–9387; d) S. Hosokawa, J. Ito, H. Nishiyama, Hisao, *Organometallics* **2010**, *29*, 5773–5775.
[26] D. Zabel, A. Schubert, G. Wolmershäuser, R. L. Jones Jr., W. R. Thiel, *Eur. J. Inorg. Chem.* **2008**, 3648–3654.
[27] a) D. Semmingsen, *Acta Chem. Scand.* **1972**, *26*, 143–154; b) F. Zou, X. Tang, Y. Huang, S. Wan, F. Lu, Z.-N. Chen, A. Wu, H. Zhang, *CrystEngComm* **2016**, *18*, 6624–6631; c) R. D. G. Jones, *J. Chem. Soc. Perkin Trans. 2* **1976**, 513–515; d) C. Prabhakar, G. B. Reddy, C. Maheedhara, R. D. Nageshwar, A. S. Devi, J. M. Babu, K. Vyas, M. R. Sarma, G. O. Reddy, *Org. Proc. Res. Dev.* **1999**, *3*, 121–125.
[28] K. Umehara, S. Kuwata, T. Ikariya, *J. Am. Chem. Soc.* **2013**, *135*, 6754–6757.
[29] a) X.-P. Li, J.-S. Zhao, S. Weng Ng, *Acta Crystallogr., Sect. E* **2010**, *66*, 1299; b) R. K. O'Reilly, V. C. Gibson, A. J. P. White, D. J. Williams, *Polyhedron* **2004**, *23*, 2921–2928; c) B. J. Cook, C.-H. Chen, M. Pink, R. L. Lord, K. G. Caulton, *Inorg. Chim. Acta* **2016**, *451*, 82–91.
[30] B. Weber, R. Betz, W. Bauer, S. Schlamp, *Z. Anorg. Allg. Chem.* **2011**, *637*, 102–107.
[31] a) M. Amberg, U. Bergsträsser, G. Stapf, J. Hartung, *J. Org. Chem.* **2008**, *73*, 3907–3910; b) M. Amberg, I. Kempter, U. Bergsträßer, G. Stapf, J. Hartung, *Tetrahedron: Asymmetry* **2011**, *22*, 752–760.
[32] a) T. Nishikubo, A. Kameyama, Y. Kimura, K. Fukuyo, *Macromolecules* **1995**, *28*, 4361–4365; b) X. Chen, Z. Lu, *Org. Lett.* **2016**, *18*, 4658–4661.
[33] M. Szewczyk, A. Bezlada, J. Mlynarski, *ChemCatChem.* **2016**, *8*, 3575–3579.
[34] W. M. Reiff, N. E. Erickson, W. A. Baker, *Inorg. Chem.* **1969**, *8*, 2019–2021.
[35] W. M. Reiff, W. A. Baker, N. E. Erickson, *J. Am. Chem. Soc.* **1968**, *90*, 4794–4800.
[36] a) V. Schünemann, H. Winkler, *Rep. Prog. Phys.* **2000**, *63*, 263–353; b) P. Gütlich, E. Bill, A. X. Trautwein, *Mössbauer Spectroscopy and Transition Metal Chemistry*, **2011**.
[37] H. P. Gunnlaugsson, *Hyperfine Interact.* **2016**, *237*, 79.
[38] A. Altomare, G. Cascarano, C. Giacovazzo, A. Guagliardi, M. C. Burla, G. Polidori, M. Camalli, *J. Appl. Crystallogr.* **1994**, *27*, 435–435.
[39] M. C. Burla, R. Caliandro, M. Camalli, B. Carrozzini, G. L. Cascarano, C. Giacovazzo, M. Mallamo, A. Mazzone, G. Polidori, R. Spagna, *J. Appl. Crystallogr.* **2012**, *45*, 351–356.
[40] G. M. Sheldrick, *Acta Crystallogr., Sect. A* **2008**, *64*, 112–122.
[41] CrysAlisPro, Agilent Technologies, Version 1.171.37.35, **2014**; CrysAlisPro, Rigaku Oxford Diffraction, Version 1.171.38.41, **2015**.

Received: November 26, 2019

